JOURNAL OF CHEMICAL INFORMATION AND MODELING

Article

pubs.acs.org/jcim

The Impact of Molecular Dynamics Sampling on the Performance of Virtual Screening against GPCRs

Ákos Tarcsay,[†] Gábor Paragi,[‡,∥] Márton Vass,[†] Balázs Jójárt,[§] Ferenc Bogár,[‡] and György M. Keserű*[,†,⊥]

[†]Discovery Chemistry, Gedeon Richter plc., 19-21 Gyömrői út, H-1103 Budapest, Hungary

[‡]MTA-SZTE Supramolecular and Nanostructured Materials Research Group, Hungarian Academy of Sciences, University of Szeged, Dóm tér 8, H-6720, Szeged, Hungary

[§]Department of Chemical Informatics, Faculty of Education, University of Szeged, Boldogasszony sgt. 6, Szeged H-6725, Hungary

Supporting Information

ABSTRACT: The formation of ligand−protein complexes requires simultaneous adaptation of the binding partners. In structure based virtual screening, high throughput docking approaches typically consider the ligand flexibility, but the conformational freedom of the protein is usually taken into account in a limited way. The goal of this study is to elaborate a methodology for incorporating protein flexibility to improve the virtual screening enrichments on GPCRs. Explicit-solvated molecular dynamics simulations (MD) were carried out in lipid bilayers to generate an ensemble of protein conformations for the X-ray structures and homology models of both aminergic and peptidergic GPCRs including the chemokine $CXCR_4$, dopamine D_3, histamine H_4, and serotonin $5HT_6$ *holo* receptor complexes. The quality of the receptor models was assessed by enrichment studies to compare X-ray structures, homology models, and snapshots from the MD trajectory. According to our results, selected frames from the MD trajectory can outperform X-ray structures and homology models in terms of enrichment factor and AUC values. Significant changes were observed considering EF1% values: comparing the original $CXCR_4$, D_3, and H_4 targets and the additional $5HT_6$ initial models to that of the best MD frame resulted in 0 to 6.7, 0.32 to 3.5 (10×), 13.3 to 26.7 (2×), and 0 to 14.1 improvements, respectively. It is worth noting that rank-average based ensemble evaluation calculated for different ensemble sizes could not improve the results further. We propose here that MD simulation can capture protein conformations representing the key interacting points of the receptor but less biased toward one specific chemotype. These conformations are useful for the identification of a "consensus" binding site with improved performance in virtual screening.

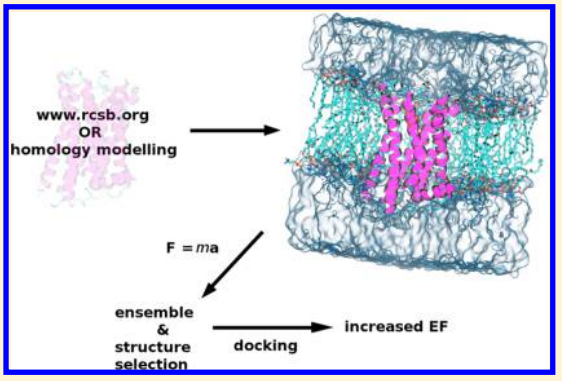

INTRODUCTION

The success of structure based virtual screening essentially depends on the accurate modeling of the physiologically relevant protein conformation.[1−3] If the appropriate conformation of the ligand−protein complex is not available for some reason, the usually applied rigid protein approach prevents either enhanced sampling of ligand conformations or the use of physically meaningful scoring functions that result in inacceptable ranking. Correspondingly, ignoring the intrinsic mobility of proteins can have a detrimental effect on the performance of virtual screening and also on structure based optimization of hits that are otherwise integral components of drug discovery programs in pharmaceutical research. Beyond the principle that proteins are not static objects—as they are typically captured with X-ray crystallography—spontaneous occurrence of discrete global fluctuations and the preset conformational equilibrium between functional states influencing ligand binding characteristics is well established.[4] According to the hypothesis of conformational selection, receptors alternate prior to ligand binding between *apo* and ligand-specific *holo* conformations.

Protein flexibility can incorporate small or large scale movements and are classified into three categories: side-chain, backbone, and domain level movements.[5] A wide variety of implementations[2,3] have been developed to model different ranges of protein flexibility such as (i) soft potentials to avoid the penalty of small steric clashes mainly for mimicking subtle side-chain movements, (ii) rotamer exploration, for higher-order side-chain movements, (iii) docking into multiple protein conformations, generally referred to as ensemble docking, (iv) hybrid methods, that incorporate backbone and side-chain movements (for example Induced Fit (IFD)[6] from Schrödinger or IFREDA[7]), and (v) postdocking pose refinement with molecular dynamics simulation.[2,3]

Among the possible implementations, ensemble docking represents a balanced approach in terms of costs and benefits.[1,3,8−10] Docking calculations are typically fast and can be run in batch parallelization that enables the use of an ensemble of protein structures. Regarding the protein

Received: February 5, 2013
Published: October 13, 2013

ACS Publications © 2013 American Chemical Society

conformations, crystallization of multiple ligand−protein complexes or *apo* structures as well as models built on NMR constraints are possible experimental sources to seed ensemble docking.[3] Although there have been several improvements in both crystallization technologies and protein crystallography, membrane proteins typically represent great challenges for experimental structure elucidation. Consequently, several key pharmaceutical targets possess only one resolved structure or can only be accessed as a comparative model.

Several computational methods are available to generate ensemble templates such as molecular dynamics simulations,[11] Monte Carlo conformational search, elastic network model simulations, or normal-mode analysis.[1−3,12,13] A fascinating proof of concept study regarding the applicability of molecular dynamics simulations of ligand−protein complex formation was recently published by Shaw and co-workers.[14] Atomistic prediction of the ligand−protein complex formation by molecular dynamics simulations of Src kinase with dasatinib[14] and β2 adrenergic receptor with its ligands[15] provided the experimentally observed binding modes. Furthermore, the activation mechanism of β2 adrenergic receptor was studied by molecular dynamics simulation of the active conformation that spontaneously transferred to the inactive crystallographically observed conformation.[16] Gloriam and co-workers simulated the transition of the inactive $5HT_{2A}$ homology model to the active state by steered molecular dynamics simulation and selected active receptor conformations for virtual screening.[17] Moreover, molecular dynamics simulations were exploited in the case of successful homology model-based virtual screening on a glucagon receptor (GLR), a family B GPCR.[18] Therefore, it is widely accepted that generation of protein conformations by the analysis of molecular dynamics trajectories reflects the physiological conditions and provides relevant seed conformations for ensemble docking. The recent advances in experimental elucidation of GPCR structures prompted us to develop a docking methodology that incorporates protein flexibility.

We have selected targets representing both aminergic and peptidergic GPCR subfamilies, namely dopamine D_3 and chemokine $CXCR_4$ receptors possessing X-ray structure as well as homology models. We were interested in the performance of our methodology in a more general context, where no X-ray structure is available; this was exemplified by the comparative model of histamine H_4 receptor that was also included among the targets. All-atom, explicit solvated MD simulations of the membrane embedded receptors were carried out to obtain different receptor conformations for docking. Initial X-ray structure, homology model, single structures form the trajectory, and the various ensembles have been compared by retrospective virtual screening using the recently published GDD ligand collection.[19] The homology model of a serotonergic target ($5HT_6$) has been developed in our laboratories during the preparation of the manuscript. Similar evaluation of the $5HT_6$ receptor model provided a further example of the utility of homology model based conformational ensembles in virtual screening.

MATERIALS AND METHODS

Receptor structures. Four systems were subjected to molecular dynamics simulation: (i) human dopamine D_3 receptor (hD3) with eticlopride (ETQ) (PDB ID: 3pbl[20]), (ii) human $CXCR_4$ chemokine receptor ($CXCR_4$) complexed with IT1t (ITD) (PDB ID: 3odu[21]), (iii) human histamine H_4 (hH_4) receptor with JNJ7777120 (JNJ) compound and $5HT_6$ with ligand SB-742457 (SB). The initial structures of the hH_4−JNJ and $5HT_6$−SB complexes were prepared by homology modeling, while in the two other cases the crystal structures were applied.

Homology Modeling of the Human Histamine H_4 Receptor. The initial homology model of the human histamine H_4 receptor was constructed with Prime 3.0[22] using the 3.1 Å resolution X-ray structure of the human histamine H_1 receptor (PDB code: 3RZE) and the sequence alignment in the Supporting Information. The N- and C-terminal peptides as well as the ICL3 were not modeled. The conformation of the F144−N147 sequence in TM4 was adjusted to resemble that of G162−S165 from the 2.4 Å resolution X-ray structure of the human β2-adrenergic receptor (PDB code: 2RH1). JNJ7777120 was first manually docked into the receptor in the binding mode described previously[23] and subjected to minimization of the 5 Å environment of the ligand with H bonds between the protonated amine and D94 and the indole NH and E182 as constraints using the default settings in MacroModel 9.9.[24] Then, JNJ7777120 was redocked into the minimized structure using Induced Fit Docking[6,25] in the Schrödinger Suite 2011 with the default settings and the same two H bonds as constraints in both docking stages. Finally, the whole structure was subjected to the Impref minimization step in the Protein Preparation Wizard.[26]

Homology Modeling of the Human $5HT_6$ Receptor. The initial homology model of the human serotonine receptor 6 was built with Prime 3.0[22] using the 2.7 Å resolution X-ray structure of the human serotonin receptor 2B (PDB code: 4IB4[28]) and the sequence alignment in the Supporting Information. The N- and C-terminal peptides as well as the ICL3 were not modeled. All the extracellular loops were refined by Prime Loop Refinement[22] using extended sampling. The SB-742457 ligand was docked to the binding site using Induced Fit Docking (IFD[6,25]). The binding site was defined using the coordinates of the original ergotamine ligand of the template. The best IFDScore complex was visually inspected and was accepted for enrichment study and MD simulation.

Molecular Dynamics Simulations. The protein−ligand complexes were immersed into a POPC membrane bilayer[29] where the number of the lipid molecules was 99. For the protein atoms ff99SB[30], for ligand and lipid molecules GAFF[31] force field parameters were assigned. The system was solvated by water molecules described by the TIP3P[32] potential. JNJ had partial charges published in ref 32; for ETQ, ITD, and SB-742457 the charges were calculated according to the *resp* protocol.[33] For ETQ, ITD, and SB-742457, conformational analysis (gas phase and MMFF94x force field[34]) was performed using the Molecular Operating Environment.[35] During partial charge calculations of the ligands, diverse conformations were selected and subjected to *ab initio* geometry optimizations at the HF/6-31G* level of theory using the Gaussian 09 software.[36] The molecular electrostatic potential was calculated at the same level of theory, and atom centered charges were calculated by means of the *resp* module of AmberTools1.5.[37] An appropriate number of Na^+ cations and Cl^- anions (25/34, 34/43, 25/30, and 25/40 for hD3-ETQ, $CXCR_4$-ITD, hH_4-JNJ, and $5HT_6$-SB-742457, respectively) were added in order to neutralize the system and mimic the ionic strength inside the cell. The force field parameters for these ions were taken from Joung and Cheatham.[38,39]

dx.doi.org/10.1021/ci400087b | J. Chem. Inf. Model. 2013, 53, 2990−2999

The molecular dynamics simulations were conducted with the NAMD 2.7 software[40] using the following protocol in order to equilibrate the membrane/water environment around the GPCR-ligand complexes:

(1) minimization (3200 steps) with restrained protein−ligand atoms (force constant was set to 10 kcal/molÅ^2)
(2) minimization (3200 steps) without restraints
(3) heating in NVT ensemble from T_i = 10 K to T_f = 310 K (in 10 steps with ΔT = 30 K and Δt = 4 ps) with restrained protein−ligand atoms (force constant was set to 10 kcal/mol Å^2)
(4) 1-ns-long MD simulation in $Np_z\gamma T$ ensemble (p_z = 1 atm, γ = 60 dyn/cm, T = 310 K, restrained protein−ligand atoms (10 kcal/mol Å^2))
(5) removing of the restraints in 10 steps with 100 ps duration of each, with linear scaling of the force constant from 1.0 to 0.0 ($Np_z\gamma T$ ensemble, p_z = 1 atm, γ = 60 dyn/cm, and T = 310 K).

After this equilibration for the hD_3-ETQ, $CXCR_4$-ITD, and $5HT_6$-SB-742457 systems, 20-ns-long simulations were conducted, which was followed by five independent (using different initial velocities), 5-ns-long MD simulations in the $Np_z\gamma T$ ensemble (p_z = 1 atm, γ = 60 dyn/cm, and T = 310 K). For the hH_4-JNJ system, distance restraints were applied between the Asp^{94}-JNJ and Glu^{182}-JNJ parallel with removing the positional restraints (step 5) because without these restraints these interactions were disrupted. Thereafter, 20-ns-long unbiased dynamics were conducted as described previously.

During the calculations, the Noosé−Hoover Langevin piston method[41,42] was used; the cutoff was set to 10 Å, and a 2/2/4 fs multistepping scheme was applied. Long range electrostatic interactions were calculated via the particle mesh Ewald method,[43] and the grid spacing was set to 1 Å.

Interacting Residues. In the present study, our goal was to identify the characteristically different binding environments of the ligands of the investigated GPCRs. Therefore, we identified those residues which have considerable interaction with the ligand during the MD simulation. The identification process was as follows. For each trajectory point, we selected those residues whose side-chain occurs in the 5 Å environment of the ligand. Then, the number of occurrences was counted along the MD trajectory for selected residues and summed up providing the cumulative occurrences. The residues were sorted according to their contribution to the cumulative occurrences (the number of occurrences of a residue divided by the cumulative occurrences multiplied by 100, in %). Starting from the top ranked residue, we summed up the contributions until reaching the value of 90%. Those residues were defined as interacting ones for a receptor which contributed to this sum. The advantage of the definition is that residues occurring only a few times in the 5 Å environment of the ligand were omitted.

Receptor Model Generation for Docking. For docking calculations, two ensembles of receptor models were generated from the MD trajectories. On one hand, structures were systematically extracted from the trajectory at the end of every nanosecond. On the other hand, receptor conformations were clustered along every individual MD trajectory, and a representative structure (model) was selected for each cluster. The former method provides around 30 models for each GPCR, while in the second case the freely adjustable parameter of the cluster selection was tuned accordingly to obtain approximately the same number of models as in the first case.

Clustering. Calculations were carried out with the ptraj program from the AmberTools[37] package. First, the structures were superimposed based on the side-chain heavy atoms of the interacting residues to the initial geometry of the trajectory concerned. Next, the "average linkage" algorithm was applied to generate clusters and representatives in each case. Clustering was based on the mass-weighted RMSD distance matrix of the same atoms as used for superposition. The number of clusters was controlled by using criteria for critical distances (ε), which was the same for all trajectories of a certain GPCR.

Docking. In the case of the H_4, D_3, and $5HT_6$ targets, the GDD ligand set was used.[19] Since a ligand set for $CXCR_4$ was not available in GDD, we reproduced the same ligand selection method as described by Cavasotto and Gatica.[19] $CXCR_4$ actives were retrieved from the Thomson Integrity[44] database, while the ZINC database[45] was used to find decoys. Finally, altogether 30 active and 1170 inactive ligands were collected. These ligands are available from the authors.

Schrödinger Suite 2012 was used for protein and ligand preparation as well as for docking. Receptor structures were prepared by the Protein Preparation Wizard,[26] including Impref minimization. Ligands were prepared by LigPrep.[46] Major tautomer and protomer states were generated by the Epik module at pH 7.4. Grids were centered on the centroid of the interacting residues. The size of the grid box was defined by the maximal ligand size of 25 Å. The dimension of the inner box—where the midpoint of the ligand must be located—was set to 14 Å along the three coordinate axes.

Docking calculations were performed by Glide[47,48] using the single precision (SP) calculation method. The default values were applied for the docking parameters except for the maximum number of minimization steps, which was set to 400. As a brief verification of the docking protocol, the original ligands were redocked into the crystal structure. These dockings provided 0.3 and 0.8 Å RMSD values considering the heavy atoms of the ligands for the D_3 (3PBL) and the $CXCR_4$ (3ODU) crystal models, respectively.

The performance of virtual screening was assessed by enrichment factor (EFx%), ROC, and AUC. The enrichment factor was defined as EFx% = $(n_{actx\%}/n_{allx\%})/(n_{act}/n_{all})$, were $n_{actx\%}$ is the number of active ligands in the top x%, $n_{allx\%}$ is the number of ranked ligands in the top x%, n_{act} is the number of all actives, and n_{all} is the total number of ligands. ROC is the plot of actives percentage versus decoys percentage in the ranked list, while AUC is the area under the ROC curve.

RESULTS AND DISCUSSION

GPCRs adopt multiple conformations ranging from the fully inactive to the active state that has crucial functional relevance from a pharmacological point of view, since partial, full, and inverse agonists or neutral antagonists have different therapeutic effects. Moreover, high affinity compounds of different chemotypes may show similar functional efficacy, suggesting that a functional state can also cover multiple protein conformations in terms of the extracellular binding pocket. The scope of this study is to investigate the potential of using multiple receptor conformations for structure based drug design purposes; therefore receptor conformations selected form MD trajectories were generated. The quality and the potential applicability of receptor conformations had been assessed by retrospective enrichment studies. The key goal was to compare high quality models that represent an optimized ligand−protein conformation (X-ray or comparative model) to

Table 1. Main Features of the Receptor Models Used in Our Study

	receptor models					
			MD details			
target	homology model	X-ray	system (ligand)	total length (ns)	number of frames *cluster*	number of frames *systematic*
$CXCR_4$	VU-MedChem[51]	3ODU	3ODU (ITD)	20 + 5 × 5 (45)	32	30
D_3	PompeuFabra[51]	3PBL	3PBL (Eticlopride)	20 + 5 × 5 (45)	30	30
H_4	this study		homology model (JNJ7777120)	20	28	21
5HT6	this study		homology model (SB-742457)	20 + 5 × 5 (45)	28	30

multiple MD frames that exhibit broader conformational variability. Three prototypic targets were investigated: $CXCR_4$, D_3, and H_4. $CXCR_4$ is a peptidergic GPCR with a large, open binding site, while D_3 and H_4 are aminergic receptors representing more closed binding pockets. Among them, D_3 and $CXCR_4$ have small-molecule bound X-ray structures. Both $CXCR_4$ and D_3 were assessed in the GPCR Dock 2010 competition; therefore the best models of the modeling community are available, and the models are entirely unbiased, since they were built before the structures were disclosed.[51] The third target is the H_4 receptor, with no reported X-ray structure. In this case, a close homologue, the H_1 receptor−ligand complex, is available,[52] which was used as a template to build a comparative model. Explicit-solvent molecular dynamics simulations of the *holo* receptors were carried out using the X-ray structures ($CXCR_4$ and D_3) or in the case of H_4, our homology model on a nanosecond time scale. *Holo* complexes were used instead of *apo* forms to prevent the collapse of the binding pocket and to preserve the steric availability of the interaction pattern of the ligand. Binding-site RMSD-based clustering and systematic sampling were used to generate approximately 30−30 receptor conformations for each target. In the case of MD, single receptor as well as ensemble evaluations were carried out. Protein flexibility was measured in terms of per residue RMSD values compared to the initial structure and presented as Supporting Information.

During the preparation of the manuscript, novel serotonin receptor structures had been published: the human $5HT_{1B}$ (4IAR[28]) and $5HT_{2B}$ (4IB4[28]). In order to provide further confirmation of our concept, we decided to evaluate an additional aminergic target from the serotonin family based on the most recent structural information. Accordingly, the $5HT_6$ homology model was built using the $5HT_{2B}$ crystal structure (4IB4[28]) as a template (having ∼35% sequence identity at TM domains compared to $5HT_6$), and the previously described protocol (20 ns equilibration and five independent 5 ns runs, interacting residues selected by their cumulative occurrences) was applied in order to test the performance of the MD-based protein conformational sampling and frame selection protocol. The SB-742457 ligand (K_i of 0.25 nM at $5HT_6$)[53] that is currently in clinical trials was docked to the binding site of the obtained homology model using the Induced Fit Docking method. This initial model was compared to the receptor models yielded by MD simulations by retrospective enrichment study using the GDD $5HT_6$ ligand set.

It should be noted that quality assessment of the different docking algorithms or the ligand sets is out of the scope of this paper. The Glide docking engine was used that has been evaluated on drug-like and fragment-sized compounds in self- and cross-docking scenarios and provided high quality results.[54−57] Therefore, we focused only on the preparation of the receptor models, from a methodological aspect. The models are summarized in Table 1.

The Impact of the Structure Source. Our primary objective was to survey the source of receptor models. The quality of receptor models had been assessed by retrospective enrichment studies that measure the feasibility of models to select active compounds from decoys. Enrichment factor, receiver operating characteristic (ROC), and area under the ROC curve (AUC) values were calculated. Our aim was to investigate whether the X-ray structure is the paramount representation of the protein conformation and the MD simulation only perturbs the protein framework and reduces its validity, or if we could find a single conformation among the MD ensemble that can outperform the experimental structure. The second objective was to assess the quality of homology models, since most of the pharmaceutically relevant GPCRs have not been crystallized to date. The H_4 target was selected as a real-life scenario, where no X-ray structure is available; thus the MD simulation is based on the homology model. During this specific assessment, the best snapshot (highest enrichment factor EF) was selected from the MD simulations regardless of whether it was found with clustering or systematic sampling. The EF and AUC results are presented in Figure 1 and in the Supporting Information.

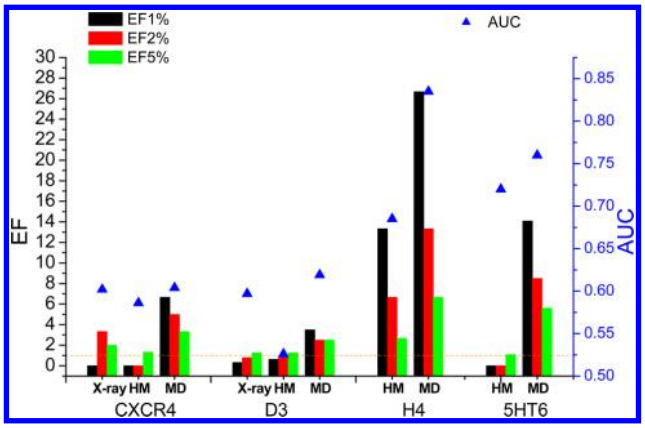

Figure 1. Enrichment factors (colored bars) and AUC values (blue triangles) for the $CXCR_4$, D_3, H_4, and $5HT_6$ targets obtained with X-ray, homology model (HM), and the best molecular dynamics frame (MD). The orange dotted line represents EF = 1. It should be noted that the *y* axis starts from EF = −1 in order to enable the representation of EF = 0 bars.

In the case of $CXCR_4$, the homology model and the X-ray structure did not result in significant enrichment. The EF1% was equal to zero (the random case produces EF1% = 1); in contrast the best MD snapshot resulted in EF1% = 6.7. Considering the aminergic D_3 receptor, the EF1% of the homology model and the X-ray was 0.63 and 0.32, respectively.

dx.doi.org/10.1021/ci400087b | J. Chem. Inf. Model. 2013, 53, 2990−2999

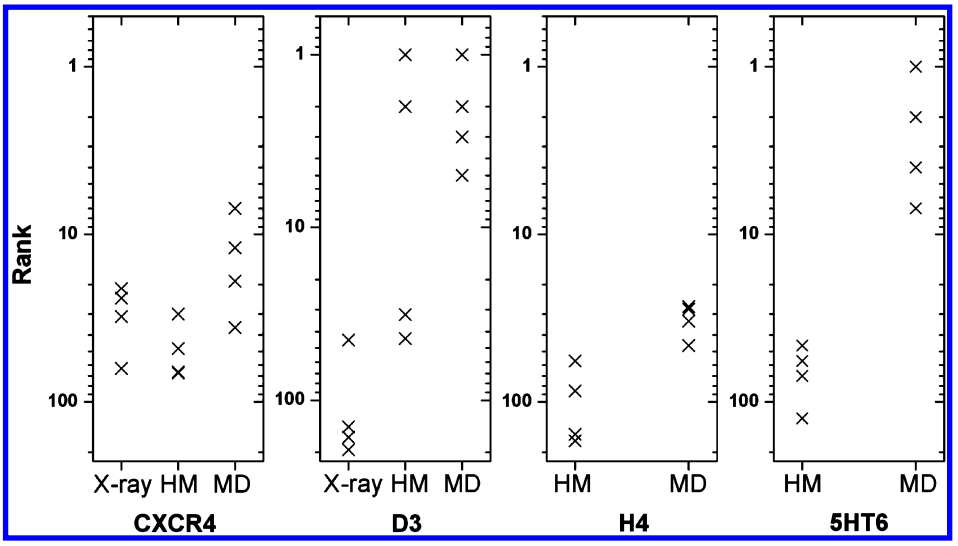

Figure 2. The ranks of the top four actives for the $CXCR_4$, D_3, H_4, and $5HT_6$ targets obtained with X-ray, homology model (HM) and the best molecular dynamics frame (MD).

In contrast, the best snapshot from the MD trajectory resulted in EF1% = 3.5. The H_4 homology model and the best MD frame yielded 13.3 and 26.7 EF1% values, respectively. In the case of the $5HT_6$ target, the homology model and the best MD frame resulted in zero and 14.1 EF1% values, respectively. The AUC values were found to be 0.72 and 0.76 for the homology model and the best MD frame, respectively. In line with the previous results, the homology model was significantly outperformed by the best MD receptor model. It is interesting to note that the MD-based docking ranked three actives among the top five compounds and five actives among the top 10; thus the performance of the MD-optimized structure was found to be very promising for prospective screening. The results of the enrichment studies of all the MD frames for the four targets and the population of clusters are presented in the Supporting Information

The results of the enrichment studies (depicted in Figure 1) can be summarized by stating that the best single structure form of the MD simulation was superior to the initial model, regardless of the target and the evaluation method (EF or AUC). This observation suggests that during the MD simulations, a "consensus" binding pocket is formed that is able to outperform the homology model or experimentally observed conformation of the protein in terms of enrichment factor. We suggest that during MD simulation of the protein–ligand complex various low-energy protein conformations are sampled, and this ensemble contains such conformations that are not entirely refined around the original ligand, but they correctly represent the interaction pattern of the binding site. Such a protein conformation is not committed to the original ligand and therefore can host and score multiple diverse active chemotypes. This hypothesis is exemplified with the four top-ranked actives in Figure 2. The top ranked active compound in case of the X-ray or homology model structures has approximately the same rank as the MD frame, but the MD frame can host multiple active compounds with similar low ranks unlike X-ray or homology models. Our hypothesis is in line with the theory of the consensus binding site refinement protocol (cIFD) that has been recently published.[58] In the case of the cIFD method, the binding site is refined around multiple active compounds simultaneously by using Locally Enhanced Sampling (LES) to preform a specific binding pocket that can host diverse actives, without steric clashes. According to our results, similar "multipotent" binding sites can be captured during MD simulation of the ligand–protein complex.

Next, we tested the robustness of the enrichment study to challenge the consensus binding site hypothesis. Because of the large number of MD frames that were included in the enrichment study, chance correlation might have occurred. In rare cases, a good enrichment might be obtained simply due to occasional scoring of some active compounds, but the whole model is not able to accommodate the actives better than inactives on average. In order to carry out statistical evaluation, the original ligand set was divided into small random subsets containing one third of the actives and one third of the decoys, and these subsets were generated 10 times for each target. During this approach, we simulated 10 enrichment studies using reduced ligand sets. However, these sets are not independent from the original; thus we consider these statistical results to be approximate. The enrichment of these small subsets was calculated, and the 10 EF1%, EF2%, EF5%, and AUC values were compared with two sample *t* tests among the homology models, X-ray structures, and best MD models. We found that the difference between homology models and X-ray structures compared to the best MD snapshots was significant ($p < 0.05$, MD was superior) for the D_3, H_4, and $5HT_6$ cases using either EF or AUC values (Supporting Information Table). In the case of $CXCR_4$, the difference between the homology model and the MD frame was significant ($p < 0.05$). Comparison of the X-ray structure and the MD frame in the case of $CXCR_4$ revealed that the difference is not significant for EF1%, EF2%, EF5%, and AUC.

Considering another aspect and assessing the applicability of comparative modeling on GPCRs, our results suggest that in the case of $CXCR_4$ and D_3, neither the X-ray nor the state of the art homology model yielded acceptable enrichment. In the cases of H_4 and $5HT_6$, where close X-ray structures were used as a template, significant enrichments were observed. The H_4 and $5HT_6$ homology model-based MD simulations resulted in a similar outcome to that of the D_3 and $CXCR_4$ cases—the MD ensemble comprised a protein model with the utmost EF—that

underlines the usefulness of comparative modeling and subsequent MD simulation on GPCRs.

It should be noted that a characteristic difference was observed between the investigated targets in terms of the overall enrichment: $CXCR_4$ and D_3 were similar to each other, but H_4 and $5HT_6$ were different. X-ray and homology models of $CXCR_4$ and D_3 resulted in lower enrichments than those of the random sampling (EF1% < 1), while the MD frames were somewhat better. Limited AUC values were observed on these targets. Planesas recently published virtual screening results using Glide with a different ligand set from that of the present study for $CXCR_4$ and achieved similar results, EF1% = 2.8 and EF5% = 4.6.[59] Cavasotto and Gatica carried out an enrichment study on D_3 using the same ligand set and obtained EF2% = 0.3, which is also similar to our results.[19] Therefore, $CXCR_4$ and D_3 might be considered as challenging targets from a structure based virtual screening aspect. In contrast, both the homology model and the MD model of H_4 yielded promising EF and AUC values. This finding is in line with the literature data; the H_4 receptor can be considered as a more tractable target yielding promising enrichments.[60,61] $5HT_6$ shows a somewhat different picture. Although, the EF value of its homology model is very poor, similarly to $CXCR_4$ and D_3, the best MD model performs considerably better.

Impact of the Binding Site Character. In order to assess the relationship between the binding site properties and enrichment values, SiteMap[62] descriptors were generated for all the MD frames for $CXCR_4$, D_3, and H_4 targets. In the case of $CXCR_4$ and D_3, we did not find significant correlation between the binding site properties and the generally low enrichment factors (Supporting Information Table). In the case of H_4, the *exposure*, *size*, *contact*, and *philic* properties (definitions are given in the Supporting Information Table) had significant correlation with EF1%, EF2%, and EF5%. The *exposure* that measures how opened the binding site is showed the highest linear correlation (0.53, 0.48, and 0.59 for EF1%, EF2%, and EF5%, respectively). Overall, the SiteMap parameters were not in a strong relationship with the enrichment values, although in the case of H_4 the *exposure* might be indicative. Thorough testing of this relationship is out of the scope of this paper.

The Impact of the Frame Selection Method. Next, we compared the two frame selection methods, namely, clustering by the binding site RMSD and the systematic sampling approaches. These collections were compared with two sample *t* tests to assess the general differences (Supporting Information Tables). No statistical difference was observed in the case of $CXCR_4$ and $5HT_6$. With regard to the D_3 target, the difference was significant for EF1%. In this case, we found the clustering method slightly better, although the EF values are unacceptable (EF1%<1). Considering EF2% and EF5% values calculated for H_4, systematic sampling performed better with statistical significance. Comparing only the best structures and using EF1% for evaluation, $CXCR_4$ enrichment values were identical (both EF1% = 6.7); for D_3, the clustering outperformed the systematic sampling (EF1% values were 3.5 and 2.5, respectively), and for H_4 and $5HT_6$, the systematic sampling surpassed the clustering (EF1% values were 27.7 and 13.3 for H_4 and 14.1 and 8.4 for $5HT_6$, respectively). Overall, clustering and systematic frame selections showed similar performance. This observation might be due to the fact that the systematic approach covered the most populated clusters, and the best frames were selected from those. The limited internal diversity of the clusters resulted in the centroid selection having a similar performance to the approximately random selection of the representatives provided by the systematic approach.

The Impact of MD Ensembles. Finally, we used the discrete protein conformations collected from MD simulations by systematic and cluster-based sampling to assess their usefulness in ensemble docking. The histogram of enrichment factors achieved at single structure evaluation revealed that for two of the targets, multiple conformations had similar high EF values among the best structures, implicating that the combination of these rankings might be beneficial (Supporting Information Table). Based on literature data, ensemble docking has typically better performance using a few carefully selected protein conformations rather than including each and every structure available.[1,63−65] Therefore, average ranks of the ligands were calculated for all the possible receptor combinations to an ensemble size up to 6. The number of enumerated ensembles is shown in Figure 3.

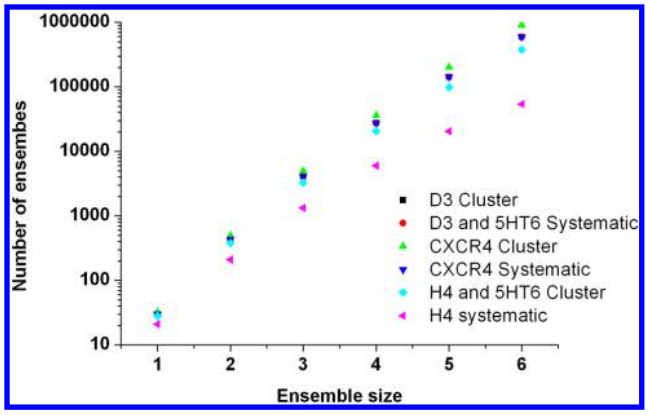

Figure 3. Number of calculated ensembles as a function of the ensemble size.

In the case of $CXCR_4$, the EF1% was better for ensemble evaluation compared to single receptor evaluation for cluster-based frame selection, but for the AUC values, no significant improvement was observed (Figure 4). Considering the D_3 and H_4 targets, the single structure enrichments could not be outperformed by ensemble evaluation. EF values obtained for $5HT_6$ suggest some limited improvement achieved by rank-average ensemble evaluation. Overall, no serious difference was observed between cluster-based and systematic MD frame selection, similarly to our previous analyses.

In summary, the rank average-based ensemble evaluation did not have an unambiguous positive effect on enrichment; however, in the cases of $CXCR_4$ and $5HT_6$, positive effects were observed considering the enrichment factor values.

Application Domain of the Proposed Methodology. Finally, we discuss the application domain of the MD-based receptor generation method proposed here to be adapted for other systems. The consensus receptor models that resulted in increased enrichment in this study had been captured by membrane-embedded MD simulations of the receptor−ligand complex. Therefore, the accuracy of the initial receptor−ligand complex has a fundamental impact on the outcome, since—in accordance with our hypothesis—during the MD simulations the binding site preserves its ligand interaction pattern; meanwhile it is equilibrated close to the energy minimum. Concurrently, several protein conformations are generated that are less biased toward the original bound ligand but projects its

dx.doi.org/10.1021/ci400087b | J. Chem. Inf. Model. 2013, 53, 2990−2999

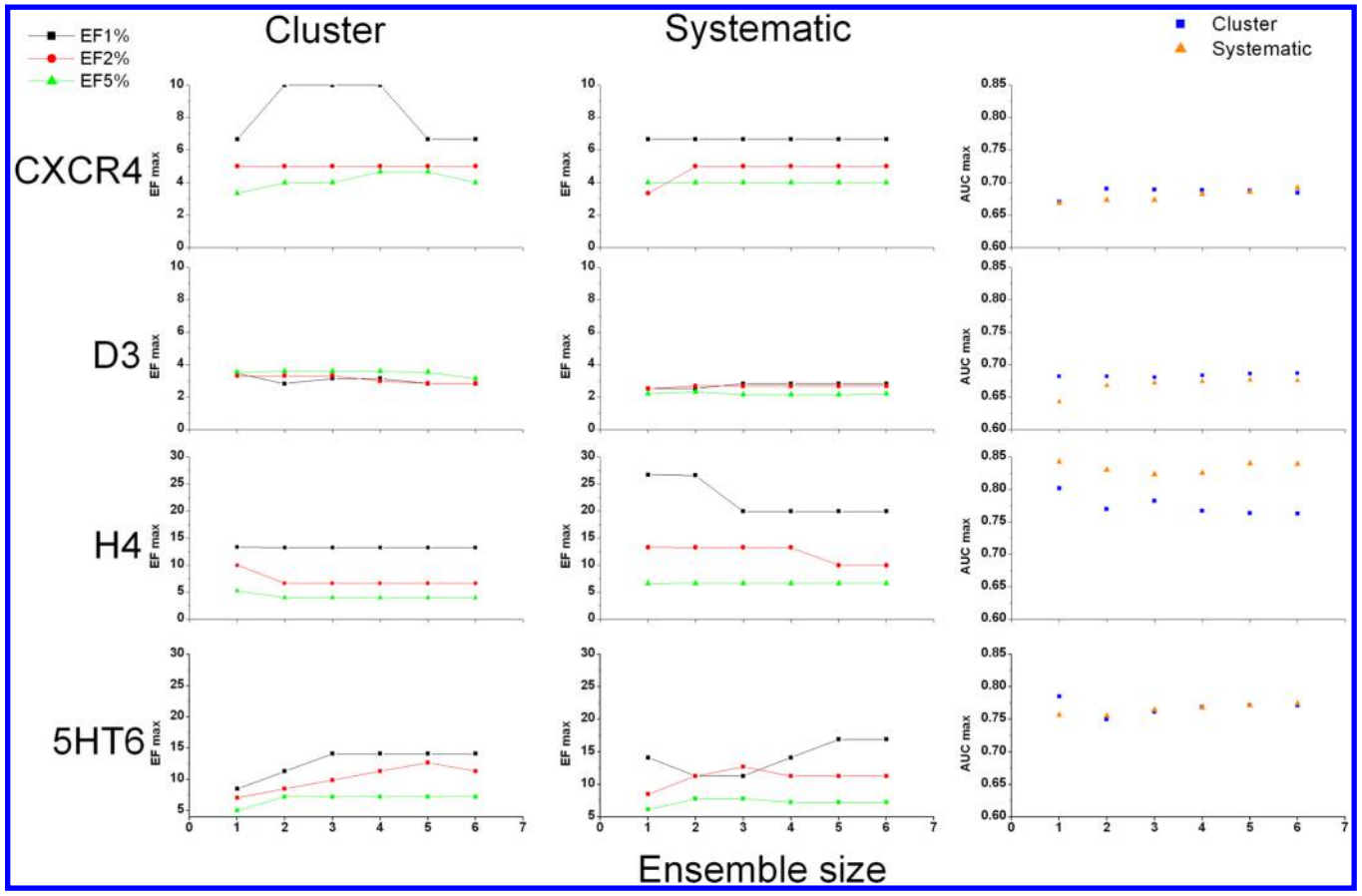

Figure 4. Best enrichment factors (EFs) and AUC values for a given ensemble size for ensemble evaluation based on rank average.

interaction surface properly. We therefore suggest using this methodology on high-quality X-ray structures (holo-form) and on those homology models that have accurately modeled complex conformation.

The GPCR Dock 2010 assessment highlighted that modeling of the D_3 receptor having 41% sequence identity with the transmembrane (TM) domain of the template β1AR satisfied the accurate modeling criteria (ligand RMSD is 0.96 Å and 58% of the contacts are reproduced).[51] In contrast, the best model of the $CXCR_4$-IT1t complex (target-template sequence identity in the TM domain is 25.5%) has a ligand RMSD of 4.88 Å, and only 36% of the contacts could be predicted correctly. In the latter case, the time scale of the MD simulations we applied here cannot ensure that the complexes find their equilibrium conformations (the backbone RMSD for the second extracellular loop of $CXCR_4$-IT1t complex was 7.42 Å for the best model). It should be noted that Shaw and co-workers have shown that homology models—in most cases—drift away from the native structure during extra long (100 μs) MD simulations.[66] In the present study, these considerations were used selecting the histamine H_4 as a modeling target, since the histamine H_1 receptor satisfied the sequence identity (~40%) for homology modeling.

Self-docking into X-ray structures and systematically built GPCR homology models yielded similar results. Aminergic GPCRs could be successfully modeled, but homology models for peptidergic GPCRs did not result in acceptable binding poses.[67] In addition, peptidergic GPCRs represent a higher level of complexity for structure-based virtual screening, as it is exemplified by hit rates for aminergic homology models compared to the peptidergic ones.[68] Our experience suggests that experimental data (X-ray or NMR) or high-quality homology models are preferred for sampling protein conformations for virtual screening applications. The protocol, however, is not recommended for more complex homology modeling cases such as peptidergic GPCRs with low quality templates.

The GPCR Dock 2010 assessment also emphasized the utility of biochemical and ligand pharmacophore information for the accomplishment of the best models. Thereby targets without known ligands (orphan receptors), or without biochemical characterization such as site directed mutagenesis, possess difficulties similar to the prediction of the correct holo complex.

In theory, the proposed methodology is not biased toward antagonist ligands and can be adapted for agonist structures as well. Because of the complexity of the functional responses of GPCRs, the level of protein flexibility incorporated in this study does not cover changes related to the activation process. Given the limited understanding of GPCR structure and function relationships to date,[27,69] we assume that structure based virtual screening can recognize ligands with high affinity to the receptor structure that should be validated first in a binding assay in vitro.

The MD simulation increases the CPU time (in our case, 4 ns/day simulation time could be achieved on 32 CPUs) resulting in the total 45 ns simulation requiring at least 10 days. According to our methodology, 20−30 receptor structures must be tested in enrichment studies that also consume computational resources. However, the computational costs of

the retrospective enrichment studies for 20−30 test conformations are still acceptable—orders of magnitude lower compared to prospective screening—considering that typically millions of compounds are virtually screened during the prospective campaigns. Although the available computational resources increased significantly during the past decade, and the MD simulations as well as the docking studies are highly parallelized, careful design of simulations still remains a principal requirement. The cost and benefit ratio should be evaluated thoroughly, but according to our study, the changes of EF1% values are encouraging: for the $CXCR_4$, D_3, and H_4 and the additional $5HT_6$ cases, the initial model compared to the best, single MD frame resulted in 0 to 6.7, 0.32 to 3.5 (10×), 13.3 to 26.7 (2×), and 0 to 14.1 improvements, respectively. This enhancement can be exploited in prospective virtual screening; therefore docking into one appropriately selected consensus receptor can replace a large number of ensemble calculations. The positive results of the very recent example, $5HT_6$, highlight the applicability of the proposed methodology in a real-life drug discovery scenario: a convincing improvement in virtual screening performance could also be achieved on a target with no experimental structure.

CONCLUSIONS

The increasing role of structure based virtual screening in hit and lead discovery demands the identification of best practices for the construction of receptor models. Accordingly, the main objective of this study was to assess the potential of single structure models and the ranking based ensemble validation to guide the selection of receptor conformations for virtual hit finding. Explicit solvent membrane dynamics simulations of four protein−ligand complexes from the GPCR family ($CXCR_4$, D_3, H_4, and $5HT_6$) were carried out to generate discrete protein conformations representing the intrinsic flexibility of the binding site. RMSD-based clustering and systematic frame selection were utilized to obtain representative conformations, and these structures were compared to X-ray structures and homology models.

According to the enrichment studies, the best single snapshots from the MD trajectory considerably outperformed the X-ray as well as the homology models. Regarding the frame selection methods, similar performance was observed. We conclude that both methods produced improved enrichments compared to the X-ray and homology model, while the ranking-based ensemble evaluation could not further increase the performance. The H_4 and $5HT_6$ cases highlighted the usefulness of homology models for MD-based receptor conformer generation, although the proposed methodology requires high quality initial protein−ligand complexes. It should also be noted that the ensemble evaluation could not outperform the best single structure at least for our selection of targets, indicating that screening on a selected single structure has an advantage over ensemble docking regarding the costs and benefits. Our results suggest that the MD simulations induce protein conformational movements that do not disrupt the accessibility of the key interacting residues. However, the formation of such binding sites that are no longer biased for the original ligand could be captured. These consensus binding pockets can host multiple diverse active ligands that accomplish the original pharmacophore pattern. On the bases of this observation, we encourage the use of MD simulation to explore the conformational space of the initial GPCR−ligand complex to create an ensemble of possible models and test their performance to find the best model for prospective screening.

ASSOCIATED CONTENT

Supporting Information

Sequence alignments, per residue RMSD values, full data of enrichment factors, AUC values, details of SiteMap descriptors, and ligand Tanimoto values. This material is available free of charge via the Internet at http://pubs.acs.org.

AUTHOR INFORMATION

Corresponding Author

*Phone: +361-438-1155. Fax: +361-438-1143. E-mail: gy.keseru@ttk.mta.hu.

Present Addresses

[‖]Department of Theoretical Chemistry, VU University Amsterdam, De Boelelaan 1083, NL-1081 HV Amsterdam, The Netherlands

[⊥]Research Centre for Natural Sciences, Hungarian Academy of Sciences, 59-67 Pusztaszeri út, H-1025 Budapest, Hungary

Funding

Notes

The authors declare no competing financial interest.

ACKNOWLEDGMENTS

This work was supported by COST Action CM1207, TÁMOP-4.2.2.C-11/1/KONV-2012-0010, and TÁMOP-4.2.2.A-11/1/KONV-2012-0047 grants.

ABBREVIATIONS

$5HT_6$, serotonin receptor type 6; AUC, area under the curve; $CXCR_4$, chemokine receptor type 4; D_3, dopamine receptor type 3; EF, enrichment factor; GPCR, G-protein coupled receptor; H_4, histamine receptor type 4; MD, molecular dynamics; ROC, receiver operator characteristic

REFERENCES

(1) Totrov, M.; Abagyan, R. Flexible ligand docking to multiple receptor conformations: a practical alternative. *Curr. Opin. Struct. Biol.* **2008**, *18*, 178−184.

(2) B-Rao, C.; Subramanian, J.; Sharma, S. D. Managing protein flexibility in docking and its applications. *Drug Discovery Today* **2009**, *14*, 394−400.

(3) Cozzini, P.; Kellogg, G. E.; Spyrakis, F.; Abraham, D. J.; Costantino, G.; Emerson, A.; Fanelli, F.; Gohlke, H.; Kuhn, L. A.; Morris, G. M.; Orozco, M.; Pertinhez, T. A.; Rizzi, M.; Sotriffer, C. A. Target flexibility: an emerging consideration in drug discovery and design. *J. Med. Chem.* **2008**, *51*, 6237−6255.

(4) Changeux, J. P.; Edelstein, S. Conformational selection or induced fit? 50 years of debate resolved. *F1000 Biol. Rep.* **2011**, *3*, 19.

(5) Teague, S. J. Implications of protein flexibility for drug discovery. *Nat. Rev. Drug Discovery* **2003**, *2*, 527−541.

(6) Sherman, W.; Day, T.; Jacobson, M. P.; Friesner, R. A.; Farid, R. Novel Procedure for Modeling Ligand/Receptor Induced Fit Effects. *J. Med. Chem.* **2006**, *49*, 534−553.

(7) Cavasotto, C. N.; Abagyan, R. A. Protein flexibility in ligand docking and virtual screening to protein kinases. *J. Mol. Biol.* **2004**, *337*, 209−225.

(8) Bottegoni, G.; Rocchia, W.; Rueda, M.; Abagyan, R.; Cavalli, A. Systematic exploitation of multiple receptor conformations for virtual ligand screening. *PLoS One* **2011**, *6*, e18845.

(9) Korb, O.; McCabe, P.; Cole, J. The ensemble performance index: an improved measure for assessing ensemble pose prediction performance. *J. Chem. Inf. Model.* **2011**, *51*, 2915−2919.

(10) Wada, M.; Kanamori, E.; Nakamura, H.; Fukunishi, Y. Selection of in silico drug screening results for G-protein-coupled receptors by using universal active probes. *J. Chem. Inf. Model.* **2011**, *51*, 2398−2407.
(11) Osguthorpe, D. J.; Sherman, W.; Hagler, A. T. Exploring protein flexibility: incorporating structural ensembles from crystal structures and simulation into virtual screening protocols. *J. Phys. Chem. B* **2012**, *116*, 6952−6959.
(12) Cavasotto, C. N.; Kovacs, J. A.; Abagyan, R. A. Representing receptor flexibility in ligand docking through relevant normal modes. *J. Am. Chem. Soc.* **2005**, *127*, 9632−9640.
(13) Rueda, M.; Bottegoni, G.; Abagyan, R. Consistent improvement of cross-docking results using binding site ensembles generated with elastic network normal modes. *J. Chem. Inf. Model.* **2009**, *49*, 716−725.
(14) Shan, Y.; Kim, E. T.; Eastwood, M. P.; Dror, R. O.; Seeliger, M. A.; Shaw, D. E. How does a drug molecule find its target binding site? *J. Am. Chem. Soc.* **2011**, *133*, 9181−9183.
(15) Dror, R. O.; Pan, A. C.; Arlow, D. H.; Borhani, D. W.; Maragakis, P.; Shan, Y.; Xu, H.; Shaw, D. E. Pathway and mechanism of drug binding to G-protein-coupled receptors. *Proc. Natl. Acad. Sci. U. S. A.* **2011**, *108*, 13118−13123.
(16) Dror, R. O.; Arlow, D. H.; Maragakis, P.; Mildorf, T. J.; Pan, A. C.; Xu, H.; Borhani, D. W.; Shaw, D. E. Activation mechanism of the *β*2-adrenergic receptor. *Proc. Natl. Acad. Sci. U. S. A.* **2011**, *108*, 18684−18689.
(17) Isberg, V.; Balle, T.; Sander, T.; Jørgensen, F. S.; Gloriam, D. E. G protein- and agonist-bound serotonin 5-HT2A receptor model activated by steered molecular dynamics simulations. *J. Chem. Inf. Model.* **2011**, *51*, 315−25.
(18) de Graaf, C.; Rein, C.; Piwnica, D.; Giordanetto, F.; Rognan, D. Structure-based discovery of allosteric modulators of two related class B G-protein-coupled receptors. *ChemMedChem.* **2011**, *6*, 2159−69.
(19) Gatica, E. A.; Cavasotto, C. N. Ligand and decoy sets for docking to G protein-coupled receptors. *J. Chem. Inf. Model.* **2012**, *52*, 1−6.
(20) Chien, E. Y.; Liu, W.; Zhao, Q.; Katritch, V.; Han, G. W.; Hanson, M. A.; Shi, L.; Newman, A. H.; Javitch, J. A.; Cherezov, V.; Stevens, R. C. Structure of the human dopamine D3 receptor in complex with a D2/D3 selective antagonist. *Science* **2010**, *330*, 1091−1095.
(21) Wu, B.; Chien, E. Y.; Mol, C. D.; Fenalti, G.; Liu, W.; Katritch, V.; Abagyan, R.; Brooun, A.; Wells, P.; Bi, F. C.; Hamel, D. J.; Kuhn, P.; Handel, T. M.; Cherezov, V.; Stevens, R. C. Structures of the CXCR4 chemokine GPCR with small-molecule and cyclic peptide antagonists. *Science* **2010**, *330*, 1066−1071.
(22) *Prime*, version 3.0; Schrödinger, LLC: New York, 2011.
(23) Lim, H. D.; de Graaf, C.; Jiang, W.; Sadek, P.; McGovern, P. M.; Istyastono, E. P.; Bakker, R. A.; de Esch, I. J.; Thurmond, R. L.; Leurs, R. Molecular determinants of ligand binding to H4R species variants. *Mol. Pharmacol.* **2010**, *77*, 734−743.
(24) *MacroModel*, version 9.9; Schrödinger, LLC: New York, 2011.
(25) Sherman, W.; Beard, H. S.; Farid, R. Use of an Induced Fit Receptor Structure in Virtual Screening. *Chem. Biol. Drug Des.* **2006**, *67*, 83.
(26) *Schrödinger Suite 2011*, Epik version 2.2; Schrödinger, LLC: New York, 2011; Impact version 5.7; Schrödinger, LLC: New York, 2011; Prime version 2.3; Schrödinger, LLC: New York, 2011.
(27) Jójárt, B.; Martinek, T. A. Performance of the General Amber Force Field in Modeling Aqueous POPC Membrane Bilayers. *J. Comput. Chem.* **2007**, *28*, 2051−2058.
(28) Wang, C.; Jiang, Y.; Ma, J.; Wu, H.; Wacker, D.; Katritch, V.; Han, G. W.; Liu, W.; Huang, X. P.; Vardy, E.; McCorvy, J. D.; Gao, X.; Zhou, X. E.; Melcher, K.; Zhang, C.; Bai, F.; Yang, H.; Yang, L.; Jiang, H.; Roth, B. L.; Cherezov, V.; Stevens, R. C.; Xu, H. E. Structural basis for molecular recognition at serotonin receptors. *Science* **2013**, *340*, 610−619.
(29) Hornak, V.; Abel, R.; Okur, A.; Strockbine, B.; Roitberg, A.; Simmerling, C. Comparison of multiple Amber force fields and development of improved. *Proteins* **2006**, *65*, 712−725.
(30) Wang, J.; Wolf, R. M.; Caldwell, J. W.; Kollamn, P. A.; Case, D. A. Development and testing of a general Amber force field. *J. Comput. Chem.* **2004**, *25*, 1157−1174.
(31) Jorgensen, W. L.; Chandrasekhar, J.; Madura, J. D.; Impey, R. W.; Klein, M. L. Comparison of simple potential functions for simulating liquid water. *J. Chem. Phys.* **1983**, *79*, 926−935.
(32) Jójárt, B.; Kiss, R.; Viskolcz, B.; Keserű, G. M. Theoretical Investigation of the Activation Mechanism of the Human Histamine H4 Receptor − An Explicit Membrane Molecular Dynamics Simulation Study. *J. Chem. Inf. Model* **2008**, *48*, 1199−1210.
(33) Bayly, C. I.; Cieplak, P.; Cornell, W. D.; Kollman, P. A. A well behaved electrostatic potential based method using charge restraints for deriving atomic charges: the RESP model. *J. Phys. Chem.* **1993**, *102*, 3787−3793.
(34) Halgren, T. A. Merck molecular force field. I. Basis, form, scope, parameterization, and performance of MMFF94. *J. Comput. Chem.* **1996**, *17*, 490−519.
(35) *Molecular Operating Environment (MOE)*, 2010.09; Chemical Computing Group, Inc.: Montreal, Quebec, Canada, 2005.
(36) Frisch, M. J.; Trucks, G. W.; Schlegel, H. B.; Scuseria, G. E.; Robb, M. A.; Cheeseman, J. R.; Scalmani, G.; Barone, V.; Mennucci, B.; Petersson, G. A.; Nakatsuji, H.; Caricato, M.; Li, X.; Hratchian, H. P.; Izmaylov, A. F.; Bloino, J.; Zheng, G.; Sonnenberg, J. L.; Hada, M.; Ehara, M.; Toyota, K.; Fukuda, R.; Hasegawa, J.; Ishida, M.; Nakajima, T.; Honda, Y.; Kitao, O.; Nakai, H.; Vreven, T.; Montgomery, J. A., Jr.; Peralta, J. E.; Ogliaro, F.; Bearpark, M.; Heyd, J. J.; Brothers, E.; Kudin, K. N.; Staroverov, V. N.; Kobayashi, R.; Normand, J.; Raghavachari, K.; Rendell, A.; Burant, J. C.; Iyengar, S. S.; Tomasi, J.; Cossi, M.; Rega, N.; Millam, J. M.; Klene, M.; Knox, J. E.; Cross, J. B.; Bakken, V.; Adamo, C.; Jaramillo, J.; Gomperts, R.; Stratmann, R. E.; Yazyev, O.; Austin, A. J.; Cammi, R.; Pomelli, C.; Ochterski, J. W.; Martin, R. L.; Morokuma, K.; Zakrzewski, V. G.; Voth, G. A.; Salvador, P.; Dannenberg, J. J.; Dapprich, S.; Daniels, A. D.; Farkas, Ö.; Foresman, J. B.; Ortiz, J. V.; Cioslowski, J.; Fox, D. J. *Gaussian 09*, revision A1; Gaussian, Inc.: Wallingford CT, 2009.
(37) Case, D. A.; Cheatham, T. E.; Darden, T., III; Gohlke, H.; Luo, R.; Merz, K. M.; Onufriev, A., Jr.; Simmerling, C.; Wang, B.; Woods, R. The Amber biomolecular simulation programs. *J. Comput. Chem.* **2005**, *26*, 1668−1688.3.
(38) Joung, S.; Cheatham, T. E. Determination of alkali and halide monovalent ion parameters for use in explicitly solvated biomolecular simulations. *J. Phys. Chem. B* **2008**, *112*, 9020−9041.
(39) Joung, I. S.; Cheatham, T. E. Molecular dynamics simulations of the dynamic and energetic properties of alkali and halide ions using water-model-specific ion parameters. *J. Phys. Chem. B* **2009**, *113*, 13279−13290.
(40) Phillips, J. C.; Braun, R.; Wang, W.; Gumbart, J.; Tajkhorshid, E.; Villa, E.; Chipot, C.; Skeel, R. D.; Kale, L.; Schulten, K. Scalable molecular dynamics with NAMD. *J. Comput. Chem.* **2005**, *26*, 1781−1802.
(41) Martyna, G. J.; Tobias, D. J.; Klein, M. L. Constant pressure molecular dynamics algorithms. *J. Chem. Phys.* **1994**, *101*, 4177−4189.
(42) Feller, S. E.; Zhang, Y.; Pastor, R. W.; Brooks, B. R. Constant pressure molecular dynamics simulation: The Langevin piston method. *J. Chem. Phys.* **1995**, *103*, 4613−4621.
(43) Darden, T.; York, D.; Pedersen, L. Particle mesh Ewald: An *N*log(*N*) method for Ewald sums in large systems. *J. Chem. Phys.* **1993**, *98*, 10089.
(44) Thomson Integrity database. http://integrity.thomson-pharma.com/integrity/xmlxsl/ (accessed 2011).
(45) Zinc database. http://zinc.docking.org/ (accessed, 2011).
(46) *LigPrep*, version 2.5; Schrödinger, LLC: New York, 2011.
(47) *Glide*, version 5.8; Schrödinger, LLC: New York, 2012.
(48) Friesner, R. A.; Banks, J. L.; Murphy, R. B.; Halgren, T. A.; Klicic, J. J.; Mainz, D. T.; Repasky, M. P.; Knoll, E. H.; Shaw, D. E.; Shelley, M.; Perry, J. K.; Francis, P.; Shenkin, P. S. Glide: A New Approach for Rapid, Accurate Docking and Scoring. 1. Method and Assessment of Docking Accuracy. *J. Med. Chem.* **2004**, *47*, 1739−1749.

(49) Halgren, T. A.; Murphy, R. B.; Friesner, R. A.; Beard, H. S.; Frye, L. L.; Pollard, W. T.; Banks, J. L. Glide: A New Approach for Rapid, Accurate Docking and Scoring. 2. Enrichment Factors in Database Screening. *J. Med. Chem.* **2004**, *47*, 1750−1759.
(50) Friesner, R. A.; Murphy, R. B.; Repasky, M. P.; Frye, L. L.; Greenwood, J. R.; Halgren, T. A.; Sanschagrin, P. C.; Mainz, D. T. Extra Precision Glide: Docking and Scoring Incorporating a Model of Hydrophobic Enclosure for Protein-Ligand Complexes. *J. Med. Chem.* **2006**, *49*, 6177−6196.
(51) Kufareva, I.; Rueda, M.; Katritch, V.; Stevens, R. C.; Abagyan, R. GPCR Dock 2010 participants Status of GPCR modeling and docking as reflected by community-wide GPCR Dock 2010 assessment. *Structure* **2011**, *19*, 1108−1126.
(52) Shimamura, T.; Shiroishi, M.; Weyand, S.; Tsujimoto, H.; Winter, G.; Katritch, V.; Abagyan, R.; Cherezov, V.; Liu, W.; Han, G. W.; Kobayashi, T.; Stevens, R. C.; Iwata, S. Structure of the human histamine H1 receptor complex with doxepin. *Nature* **2011**, *475*, 65−70.
(53) Upton, N.; Chuang, T. T.; Hunter, A. J.; Virley, D. J. 5-HT6 receptor antagonists as novel cognitive enhancing agents for Alzheimer's disease. *Neurotherapeutics.* **2008**, *5*, 458−69.
(54) Sándor, M.; Kiss, R.; Keserű, G. M. Virtual fragment docking by Glide: a validation study on 190 protein-fragment complexes. *J. Chem. Inf. Model.* **2010**, *50*, 1165−72.
(55) McGann, M. FRED pose prediction and virtual screening accuracy. *J. Chem. Inf. Model.* **2011**, *51*, 578−96.
(56) Cross, J. B.; Thompson, D. C.; Rai, B. K.; Baber, J. C.; Fan, K. Y.; Hu, Y.; Humblet, C. Comparison of several molecular docking programs: pose prediction and virtual screening accuracy. *J. Chem. Inf. Model.* **2009**, *49*, 1455−1474.
(57) Repasky, M. P.; Murphy, R. B.; Banks, J. L.; Greenwood, J. R.; Tubert-Brohman, I.; Bhat, S.; Friesner, R. A. Docking performance of the glide program as evaluated on the Astex and DUD datasets: a complete set of glide SP results and selected results for a new scoring function integrating WaterMap and glide. *J. Comput.-Aided Mol. Des.* **2012**, *26*, 787−799.
(58) Kalid, O.; Toledo Warshaviak, D.; Shechter, S.; Sherman, W.; Shacham, S. Consensus Induced Fit Docking (cIFD): methodology, validation, and application to the discovery of novel Crm1 inhibitors. *J. Comput.-Aided Mol. Des.* **2012**, *26*, 1217−1228.
(59) Planesas, J. M.; Pérez-Nueno, V. I.; Borrell, J. I.; Teixidó, J. Impact of the CXCR4 structure on docking-based virtual screening of HIV entry inhibitors. *J. Mol. Graphics Model.* **2012**, *38*, 123−36.
(60) Kiss, R.; Noszál, B.; Rácz, A.; Falus, A.; Eros, D.; Keserű, G. M. Binding mode analysis and enrichment studies on homology models of the human histamine H4 receptor. *Eur. J. Med. Chem.* **2008**, *43*, 1059−1070.
(61) Kiss, R.; Kiss, B.; Könczöl, A.; Szalai, F.; Jelinek, I.; László, V.; Noszál, B.; Falus, A.; Keserű, G. M. Discovery of novel human histamine H4 receptor ligands by large-scale structure-based virtual screening. *J. Med. Chem.* **2008**, *51*, 3145−3153.
(62) *SiteMap*, version 2.5; Schrödinger, LLC: New York, 2011.
(63) Rueda, M.; Bottegoni, G.; Abagyan, R. Recipes for the selection of experimental protein conformations for virtual screening. *J. Chem. Inf. Model.* **2010**, *50*, 186−193.
(64) Korb, O.; Olsson, T. S.; Bowden, S. J.; Hall, R. J.; Verdonk, M. L.; Liebeschuetz, J. W.; Cole, J. C. Potential and limitations of ensemble docking. *J. Chem. Inf. Model.* **2012**, *52*, 1262−1274.
(65) Xu, M.; Lill, M. A. Utilizing experimental data for reducing ensemble size in flexible-protein docking. *J. Chem. Inf. Model* **2012**, *52*, 187−198.
(66) Raval, A.; Piana, S.; Eastwood, M. P.; Dror, R. O.; Shaw, D. E. Refinement of protein structure homology models via long, all-atom molecular dynamics simulations. *Proteins* **2012**, *80*, 2071−9.
(67) Beuming, T.; Sherman, W. Current assessment of docking into GPCR crystal structures and homology models: successes, challenges, and guidelines. *J. Chem. Inf. Model.* **2012**, *52*, 3263−3277.
(68) de Graaf, C.; Kooistra, A. J.; Vischer, H. F.; Katritch, V.; Kuijer, M.; Shiroishi, M.; Iwata, S.; Shimamura, T.; Stevens, R. C.; de Esch, I. J.; Leurs, R. Crystal structure-based virtual screening for fragment-like ligands of the human histamine H(1) receptor. *J. Med. Chem.* **2011**, *54*, 8195−206.
(69) Wacker, D.; Wang, C.; Katritch, V.; Han, G. W.; Huang, X. P.; Vardy, E.; McCorvy, J. D.; Jiang, Y.; Chu, M.; Siu, F. Y.; Liu, W.; Xu, H. E.; Cherezov, V.; Roth, B. L.; Stevens, R. C. Structural features for functional selectivity at serotonin receptors. *Science* **2013**, *340*, 615−619.